Hydrol. Earth Syst. Sci. Discuss., 8, 715–761, 2011
www.hydrol-earth-syst-sci-discuss.net/8/715/2011/
doi:10.5194/hessd-8-715-2011

Hydrology and Earth System Sciences Discussions

An operational hydrological ensemble prediction system for the city of Zurich (Switzerland): skill, case studies and scenarios

N. Addor[1,2], S. Jaun[1,3], and M. Zappa[1]

[1]WSL Swiss Federal Institute for Forest, Snow and Landscape Research, Birmensdorf, Switzerland
[2]Institute for Atmospheric and Climate Science, ETH Zurich, Zurich, Switzerland
[3]Swiss Federal Office for the Environment, Ittigen, Switzerland

Received: 30 September 2010 – Accepted: 9 January 2011 – Published: 20 January 2011

Correspondence to: N. Addor (nans.addor@alumni.ethz.ch)

Published by Copernicus Publications on behalf of the European Geosciences Union.

Abstract

The Sihl River flows through Zurich, Switzerland's most populated city, for which it represents the largest flood threat. To anticipate extreme discharge events and provide decision support in case of flood risk, a hydrometeorological ensemble prediction system (HEPS) was launched operationally in 2008. This models chain relies on limited-area atmospheric forecasts provided by the deterministic model COSMO-7 and the probabilistic model COSMO-LEPS. These atmospheric forecasts are used to force a semi-distributed hydrological model (PREVAH), coupled to a hydraulic model (FLORIS). The resulting hydrological forecasts are eventually communicated to the stakeholders involved in the Sihl discharge management. This fully operational setting provides a real framework to compare the potential of deterministic and probabilistic discharge forecasts for flood mitigation.

To study the suitability of HEPS for small-scale basins and to quantify the added-value conveyed by the probability information, a reforecast was made for the period June 2007 to December 2009 for the Sihl catchment (336 km^2). Several metrics support the conclusion that the performance gain can be of up to 2 days lead time for the catchment considered. Brier skill scores show that COSMO-LEPS-based hydrological forecasts overall outperform their COSMO–7 based counterparts for all the lead times and event intensities considered. The small size of the Sihl catchment does not prevent skillful discharge forecasts, but makes them particularly dependent on correct precipitation forecasts, as shown by comparisons with a reference run driven by observed meteorological parameters. Our evaluation stresses that the capacity of the model to provide confident and reliable mid-term probability forecasts for high discharges is limited. The two most intense events of the study period are investigated utilising a novel graphical representation of probability forecasts and used to generate high discharge scenarios. They highlight challenges for making decisions on the basis of hydrological predictions, and indicate the need for a tool to be used in addition to forecasts to compare the different mitigation actions possible in the Sihl catchment.

HESSD
8, 715–761, 2011

An operational HEPS for the city of Zurich: skill, case studies and scenarios

N. Addor et al.

1 Introduction

1.1 Decision-making based on atmospheric and hydrological forecasts

To effectively anticipate and mitigate weather-related impacts, strategies that take into account climatological records or meteorological forecasts have been developed in recent decades. The first scientific studies published in the 1970s–1980s showed that an efficient use of weather and climate information could provide an added-value in diverse fields and decision-making situations (e.g. the review by Katz and Murphy, 1997). Novel opportunities and challenges were provided in the 1990s by the introduction of global atmospheric ensemble prediction systems (EPS, e.g. Molteni et al., 1996) and more recently by their downscaled limited-area derivatives (e.g. COSMO-LEPS, Marsigli et al., 2005). Ensembles are composed of several members, starting from slightly perturbed initial conditions, and aim to reflect the predictability of atmospheric conditions through the amount of spread among their members. Reliable EPS enable the estimation of the probability of local weather events, and are expected to deliver a more trustworthy basis for quantifying risk and providing early warnings than their deterministic counterparts. Among others, Richardson (2000) and Zhu et al. (2002) have investigated their benefits in the domain of decision-making using a simple cost-loss ratio model. They reported that, in comparison with deterministic forecasts, probabilistic forecasts offer an added-value for a wider range of end-users and present a higher economic value for the majority of end-users and lead-times. However, the ability of the standard two-action, two-event cost-loss ratio scheme to effectively assist with real decision-making situations is disputed (e.g. Murphy, 1985).

When coupled to a hydrological model, an EPS forms a hydrological ensemble prediction system (HEPS). HEPS have developed rapidly in the last few years (see the review by Cloke and Pappenberger, 2009). They have been adopted by several flood forecast centres and are, for example, routinely run by the European Flood Alert System (EFAS) of the European Commission Joint Research Centre (Thielen et al., 2009a). An evaluation of two years of EFAS forecasts for Europe suggests the results are promising, especially when accounting for forecast persistence (Bartholmes et al., 2009). On a smaller scale, the Swiss Federal Office for the Environment (FOEN) operationally runs deterministic and probabilistic hydrological forecasts for the Swiss part of the Rhine basin (Zappa et al., 2008). In the framework of the Mesoscale Alpine Programme (MAP), a demonstration of probabilistic hydrological and atmospheric simulation of flood events in the Alpine region (D-PHASE) was performed. The feasibility of a real-time hydrological forecast system that combines radar-based, high-resolution and ensemble hydrological forecasts is shown, and examples illustrating the usefulness of the probability information are provided (Zappa et al., 2008; Rotach et al., 2009). End-user feedback has so far been positive.

Considerable efforts have been made to demonstrate and quantify the added-value provided by HEPS, as illustrated by the following examples. Verbunt et al. (2007) analysed qualitatively two severe discharge events, in the upper Rhine basin and in central Europe. These were missed by deterministic runoff predictions but adequately forecast by probabilistic forecasts. The authors report good probabilistic forecast guidance up to 48 h lead time for the two investigated cases. For August 2005 flood event in the upper Rhine basin, Jaun et al. (2008) highlight that forecast uncertainty as reflected by ensemble dispersion provides additional guidance in comparison to deterministic forecasts. This is in particular supported by higher Brier skill scores. Velázquez et al. (2009) compared, for a rainfall event in Quebec, the continuous ranked probability score of an hydrological ensemble with the absolute error of a deterministic forecast and concluded that the probability information led to a performance gain. First attempts to evaluate probabilistic discharge forecast from an economics perspective (Roulin, 2007) relied on a cost-loss ratio-based decision model and showed that hydrological ensemble predictions have greater skills than deterministic ones. Laio and Tamea (2007) proposed new tools for economical evaluation of probability discharge forecasts, but emphasize that the choice of the therefore necessary cost-loss functions is subjective and may be disputed. Reggiani et al. (2009) suggested a stirring approach consisting in combining calibrated probabilistic forecasts to cost-loss functions to estimate economic risk, computed as the expected cost.

1.2 Discharge monitoring and flood mitigation in the Sihl catchment

The Sihl catchment originates in the Swiss Alps (Fig. 1) and drains basins which are particularly prone to flash floods. In winter snow accumulates in the headwaters. Snow melt governs runoff generation in late spring and early summer. The Sihl River flows through Zurich, the most populated city in Switzerland. Shortly before joining the larger Limmat River, the Sihl flows beneath the main railway station of Zurich (Fig. 2).

Although the area was comparatively little affected by the devastating floods of August 2005 (Bezzola and Hegg, 2007, 2008; Jaun et al., 2008), these floods prompted a series of studies assessing the flood risk of the catchment (Schwanbeck et al., 2007). Floods are especially threatening while a new underground railway station, located below the river bed, is being built (Bruen et al., 2010). Two tide gates have been installed in the river bed for the duration of the project (2008–2011) (Fig. 2). They provide dry construction areas, but therefore reduce the section available for the river by around 40%.

To cope with the resulting increased flood risk, the Department of Waste, Water, Energy and Air (AWEL) of Canton Zurich requested the Swiss Federal Railway (SBB) to organize a panel of experts. This panel is in charge of monitoring the Sihl discharge, of representing the interests of the stakeholders concerned by the river, and of setting up an emergency procedure to mitigate flooding events. A first mitigation measure is the preventive controlled water release (drawdown) from the Lake Sihl, which collects the waters from a 156 km^2 large headwater (Fig. 1). Drawdowns are designed to increase the buffering capacity of the lake in case of floods. Secondly, should the Sihl discharge exceed 300 m^3/s, the gates sealing the two channels beneath the main railway station can be opened, giving the river bed its full capacity. This would result in the inundation of the construction site, but it would reduce the risk of flooding the areas around Zurich main railway station. To improve decision support for the panel of experts, the Swiss

HESSD
8, 715–761, 2011

Federal Institute for Forest, Snow and Landscape Research (WSL) was mandated to implement an ensemble flood forecasting system. This constitutes the corner stone of this study. More details on the Sihl catchment, the flood-warning procedures and the mitigation measures can be found in Badoux et al. (2010).

1.3 Scope of the present paper

This study concentrates on the evaluation of the operational streamflow forecasting system of the Sihl catchment for a 31-month reforecast period. The evaluation was in particular tailored to cope with the weaknesses identified in the review paper by Cloke and Pappenberger (2009) and strives following objectives: (1) to compare quantitatively probabilistic and deterministic hydrological forecasts to assess whether the former has added-value over the latter, (2) to discriminate between errors originating from atmospheric forecasts and those stemming from the hydrological/hydraulic components of the models chain, (3) to analyse the reliability of the forecasts, ensemble members' dispersion, hit rate and false alarm ratio, (4) to obtain some insights into the performance of the flood prediction chain by analysing the two most severe events during the study period (one of which being a forecast failure), and (5) to investigate extreme discharge scenarios.

This paper differs from similar studies in the nature of the catchment investigated. It has a total area of 336 km^2, which is considerably smaller than most catchments, and even sub-catchments, referred to in the current literature on ensemble streamflow forecasting (e.g. Dietrich et al., 2008; Jaun and Ahrens, 2009; Thielen et al., 2009b; Reggiani et al., 2009). The current state of knowledge for larger basins suggests that the skill of ensemble prediction systems improves with increasing catchment size (Renner et al., 2009). Furthermore, forecast uncertainty is reported to decline with increasing catchment size (Jaun et al., 2008). The usefulness of such systems in small mesoscale areas has not been yet assessed and therefore we focus on the skill of an operational HEPS for comparatively small catchment. Furthermore, the reservoir lake required the implementation of a module to account for the consequences of possible lake drawdowns, overflow and hydropower production on the discharge in Zurich. In this basin, correct assessment of events leading to snow accumulation and snow melt is crucial for obtaining good forecasts from October to May. Finally, the pre-alpine topography of the region and the presence of sub-catchments prone to flash floods triggered by summer thunderstorms complicate correct meteorological and hydrological modeling.

This paper also explores how flood mitigation measures could be triggered on the basis of the presented streamflow forecasts. The operational setting the Sihl catchment enables to illustrate the complexity of such a decision process involving imperfect forecasts (Bruen et al., 2010).

2 The hydrological ensemble prediction system

2.1 Probabilistic and deterministic atmospheric models

As the operational hydrological forecasts for the Sihl catchment are not systematically archived, a reforecast from June 2007 to December 2009 was completed to proceed with model evaluation. Runs in hindcast mode were issued from a recent model version (November 2009), using operationally available information only. The prediction chain is sketched out in Fig. 3 and described below.

Probability atmospheric forecasts are based on the global Ensemble Prediction System (EPS, Molteni et al., 1996) of the European Centre for Medium-Range Weather Forecasts (ECMWF), which is issued twice daily. The two youngest runs of this model are combined to form a super-ensemble of 102 members (Marsigli et al., 2005), from which 16 representative members are selected. They are dynamically downscaled on a daily basis from their original ~50 km horizontal resolution to a ~10 km resolution (~7 km since December 2009). This is performed by the Limited-area Ensemble Prediction System developed and run by the COnsortium for Small-scale MOdelling (COSMO-LEPS, Molteni et al., 2001). COSMO-LEPS relies on the non-hydrostatic

HESSD
8, 715–761, 2011

COSMO model (Steppeler et al., 2003) run with initial and boundary conditions provided by the representative members. Hydrological forecasts for the Rhine catchment have been shown to improve after this dynamic downscaling (Renner et al., 2009).

The lead time of COSMO-LEPS is of 132 h, with three-hourly output intervals. Forecasts are initialized at 12:00 UTC and are delivered approximately 10 h later. As the hydrological model requires initialization at 00:00, the first 12 h of the atmospheric ensemble forecasts are disregarded and 120 h of hydrological forecasts are computed. This cutoff is consistent with the temporal data availability in operational mode. Note that, while errors in streamflow forecasts have multiple sources, the present ensemble principally aims to capture and cascade the uncertainty arising from initial atmospheric conditions, as they are commonly regarded as the most important error factor in hydrological forecasts. To account for some of the model uncertainty, the convection scheme (Marsigli et al., 2005) is randomly chosen at each COSMO-LEPS integration. Similarly, the value of two model parameters (the maximal turbulent length scale and the length scale of thermal surface patterns) is randomly chosen from a set of two reasonable values for each variable.

Deterministic atmospheric forecasts are obtained from the operational model COSMO-7, the Swiss Federal Office of Meteorology and Climatology (MeteoSwiss) implementation of COSMO model. COSMO-7 is nested in ECMWF deterministic global model and presents a horizontal grid spacing of ~7 km. It offers a total time horizon of 72 h. During the study period, COSMO-7 forecasts are issued twice a day (at 00:00 UTC and 12:00 UTC). However, only the forecasts from the 00:00 UTC run are here considered. In contrast to COSMO-LEPS, no random selection of a parametrization or a parameter value is applied to reflect model uncertainty.

Forecasts of temperature, precipitation, wind, relative humidity, sunshine duration and global radiation are downscaled for both atmospheric models to a resolution of 500 m to meet the grid-size requirements of the hydrological model, as described in Jaun et al. (2008).

HESSD
8, 715–761, 2011

2.2 Hydrological and hydraulic models

The downscaled atmospheric forecasts are used to force the semi-distributed hydrological modelling system PREVAH (PREecipitation-Runoff-EVApotranspiration HRU Model). PREVAH is a conceptual hydrological model and clusters raster grids of similar hydrological properties into hydrologic response units (HRU, Gurtz et al., 1999). For the Sihl catchment, one HRU averages about 7 raster cells of $500 \times 500\,m^2$. Details on PREVAH input data, structure, parameterizations and tools can be found in Viviroli et al. (2009b).

The hydrological model calibration and evaluation for the Sihl catchment was performed by Schwanbeck et al. (2007), with the catchment split into nine sub-catchments (Fig. 1). This discretization enables in particular a simple representation of water management of the Sihl reservoir.

The sub-catchments of Alp, Biber, Minster and the sub-catchment downstream of the gauge Blattwag were calibrated on the basis of the observed runoff time series. The parameters for the other sub-basins were regionalised on the basis of the five most similar calibrated catchments out of a database of 140 successfully calibrated Swiss catchments (Viviroli et al., 2009a,c). The chosen calibration method is a intermediate solution between a flood-oriented and average discharge-oriented optimization (Viviroli et al., 2009a). Validation (Schwanbeck et al., 2007) revealed a tendency towards volume overestimation but an overall satisfying peak discharge representation.

Initial conditions for PREVAH are provided by a hydrological reference simulation (HREF) driven by interpolated observations from weather stations (see Fig. 1 for the location of the rain-gauges). Note that HREF was also used to identify the origin of forecasts errors. To focus on meteorological uncertainties, the forecasts were compared with HREF instead of with observations (OBS). This removes most of the error introduced by PREVAH and the subsequent hydraulic model. For instance, if OBS and HREF correspond well, while the hydrological forecast overestimates OBS, this overestimation was probably introduced by the atmospheric model.

HESSD
8, 715–761, 2011

An operational HEPS for the city of Zurich: skill, case studies and scenarios

N. Addor et al.

PREVAH forecasts are combined with observations of the level of the Lake Sihl for a sound water balance of the artificial lake. This module accounts principally for (1) estimations of the hydropower production, (2) the eventual triggering of the dam emergency regulation (water is released from the lake into the Sihl if its level rises more than two centimeters within 30 min) and (3) water overspill if the lake operation limit (889.34 m a.s.l.) is exceeded. See Badoux et al. (2010) for more details on dam regulation.

Because of the elongated shape of the basin between Blattwag and Zurich (Fig. 1), a hydraulic model was used to propagate the flood wave. Routing is carried out by the hydraulic model FLORIS, a commercial 1-D simulation program developed in the 1990s by the Laboratory of Hydraulics, Hydrology and Glaciology (VAW) of the ETH Zurich. FLORIS computes possible Lake Sihl overflows and delivers forecasts of the timing and discharge of the flood wave originating from the PREVAH sub-catchments, combined to eventual water release from the Lake Sihl.

3 Model evaluation from three perspectives

A major issue faced by this study was the under-sampling due to the low number of severe events. A comparison between the duration of the reforecast period (∼ 2.5 years) and the return period of discharge events for which large driftwoods reach Zurich (∼30 years, 250 m^3/s) suffices to illustrate that even a reforecast of several decades would not present enough extreme events to build robust statistics. To cope with this well known limitation in evaluation of HEPS, three complementary perspectives were chosen.

First, HEPS skills to forecast low to high discharges were evaluated using several metrics and graphical representations. Although these results cannot be directly extrapolated for extreme discharges, it is argued that they can highlight those deficiencies in the models chain that may also also affect extreme discharges forecasts. Second, COSMO-7- and COSMO-LEPS-based forecasts for the two most intense events of the

HESSD
8, 715–761, 2011

study period were analysed and compared. The insights provided by this case-by-case analysis are limited because none of these events exceeded the first critical threshold of 250 m^3/s. This makes assessing model's performance for events endangering the city of Zurich delicate. To overcome this, a third perspective was explored. Two scenarios with increased lake level were computed. They led to overspills of the Lake Sihl, resulting in increased discharges in Zurich. These three approaches are described in the next three sub-sections.

3.1 Evaluation of low to high discharge forecasts

For the evaluation of the year-round model performance, the Nash-Sutcliffe efficiency NSE (Nash and Sutcliffe, 1970) and the volume error VOL (as formulated in Zappa and Kan, 2007) were selected because they enable fast comparison with other studies due to their widespread use in evaluation of hydrological models. The mean absolute error MAE (Wilks, 2006) was also chosen as it is easily interpretable and enables the contribution of some error sources within the forecast chain to be assessed quantitatively. As these three indices are designed for deterministic forecasts, COSMO-LEPS forecasts were reduced to their median to be evaluated. Note that a large part of the ensemble information is thereby disregarded and hence theses scores do not capture the information content of the full ensemble. Attention was focused on the level of the Lake Sihl and on the Sihl discharge in Zurich, as these two variables are of most interest for the end-users.

For the VOL computation, hourly values were used. In contrast, for NSE, MAE and all the scores discussed below, evaluations were based on observed and simulated daily maxima. Different lead times from 1 day (1–24 h) to 5 days (97–120 h), referred to as LT1 to LT5 subsequently, were considered. For COSMO-7, LT1 to LT3 were assessed while for COSMO-LEPS, LT1 to LT5 were evaluated to take into account the models' respective time horizons.

Different discharge thresholds were considered (Table 1). They consist of the 75th, 90th and 99th quantiles of the daily maximum distribution estimated from records of

HESSD
8, 715–761, 2011

hourly measurements from 1974 to 2007 in Zurich. They represent a trade-off between low thresholds (e.g. the average discharge) and very high thresholds (e.g. associated with a return period of 100 years or more). The former would lead to an evaluation largely irrelevant for flood forecasting purposes and the latter to weak statistics, given the duration of the present reforecast.

To compare the performance of deterministic and probabilistic forecasts, the Brier skill score (BSS) was chosen (e.g. Wilks, 2006). This skill score has the advantage that it can be applied to both deterministic and probabilistic forecasts, without requiring the transformation of a probability forecast into a deterministic one (e.g. by considering the median only). It corresponds to a ranked probability skill score (RPSS, Wilks, 2006) for a single threshold, and hence allows for the individual evaluation of several discharge thresholds. BSS is based on the Brier score (BS), which can be seen as a mean squared error of probabilities, and reads:

$$\mathrm{BS} = \frac{1}{n}\sum_{d=1}^{n}(o_\mathrm{d} - y_\mathrm{d})^2 \tag{1}$$

where n is the number of days of the reforecast. o_d (resp. y_d) indicates whether the daily maximum of the observation (resp. of COSMO-7) exceeded the threshold considered (1 = yes, 0 = no). For the probabilistic COSMO-LEPS, y_d is the probability of exceeding this threshold. In this study, such probabilities were computed as the number of ensemble members exceeding the threshold divided by the total number of members (16, i.e. ensemble members were not weighted). Forecasts show a null BS if they are perfect and a positive BS otherwise. The combination of the obtained BS with the BS of a climatology forecast (BS_ref) and of a perfect forecast ($\mathrm{BS}_\mathrm{perf} = 0$) yields

$$\mathrm{BSS} = 1 - \frac{\mathrm{BS}}{\mathrm{BS}_\mathrm{ref}}. \tag{2}$$

A BSS of 1 designates perfect forecasts, while positive BSS correspond to forecasts with more skill than the reference. As we are interested in investigating the actual

HESSD
8, 715–761, 2011

and not the potential model performance, the negative BSS bias associated with small ensemble size was not removed (Weigel et al., 2007). To evaluate the influence of the limited number of high intensity events on BSS, confidence intervals were derived by bootstrapping. 500 random samples of 940 daily maxima pairs of forecast-observations were drawn with replacement from the 940 days of the study period. The BSS was then computed for each bootstrap sample, enabling an estimation of a confidence interval formed by the 5% and 95% quantiles.

When using a probability forecast, a common way to decide whether or not to issue a warning is based on thresholds exceedance. This requires the definition of a probability threshold P (e.g. 60%) and a weather or hydrological threshold Q (e.g. a discharge of 250 m^3/s in Zurich). If the forecast probability to exceed Q is greater than P, a decision to implement protection measures may be taken. A challenge here consists in finding a balance between a risk-adverse strategy (e.g. a low P might frequently lead to unnecessary preventive measures) and a risk-friendly strategy (e.g. a high P might lead to missing an extreme event). This dilemma is illustrated by the variation in the hit rate H and false alarm rate F (Eqs. 3 and 4) with P as summarized by relative operating characteristics curves (ROC, Mason, 1982).

$$H = \frac{h}{h+m} = \frac{\text{hits}}{\text{observed events}}, \tag{3}$$

$$F = \frac{f}{f+c} = \frac{\text{false alarms}}{\text{non}-\text{events}}, \tag{4}$$

where h is the number of hits, m the number of misses, f the number of false alarms and c the number of correct rejections during the study period. h, m, f and c are defined using a contingency table (e.g. Zhu et al., 2002).

In forecasting of extreme events, false alarms are considerably less frequent than correct rejections, as highlighted by the well known Finley case for evaluating tornadoes (Murphy, 1996). Therefore, even false alarm prone systems can benefit from a low F. In contrast, the false alarm ratio FAR (Eq. 5) does not reward correct rejections, and hence can be considered as a more informative metric on the frequency of false alarms for severe events (Ambühl, 2010). FAR was therefore preferred to F in this study to produce ROC.

$$\mathrm{FAR} = \frac{f}{f+h} = \frac{\text{false alarms}}{\text{forecast events}} \quad (5)$$

HREF and COSMO-7 forecasts were considered as binary forecasts (i.e. exceedance or not of the discharge threshold by the daily maximum) to compute corresponding H and FAR.

Reliability diagrams enable in particular the assessment of model reliability, i.e. of the correspondence between the forecast probability and the observed relative frequency (e.g. Wilks, 2006). The diagram associated with reliable forecasts follows the plot diagonal.

Rank diagrams show the rank of OBS (resp. of HREF) within the ensemble members (Anderson, 1996). They highlight whether the consistency condition is met, i.e. whether the ensemble includes OBS (resp. HREF) being predicted as an equiprobable member. If it does, the rank histogram has an uniform distribution. Other histogram shapes indicate over- or underdispersion tendencies and model biases (see Wilks, 2006, for examples).

3.2 Visualisation of case studies using continuous persistence plots

For the evaluation of the forecasts for the two most intense events of the study period, a novel representation of probabilistic forecasts is proposed. Similarly to persistence plots (e.g. Thielen et al., 2009b), this new type of plot shows how the predictions of a given event evolve over time, by displaying the outputs from several model runs on the same graph.

However, while for each realisation of the model, persistence plots usually display one forecast threshold exceedance per day of forecast, hourly values of selected quantiles are depicted by these plots. In this article, the ensemble minimum and maximum,

HESSD
8, 715–761, 2011

as well as the 25% and the 75% quantiles, were chosen. We argue that this kind of plot enables a finer and more quantitative comparison of the model runs because (1) it is based on hourly instead of daily values and (2) the four quantiles chosen are considered to reflect with more details the PDF of the HEPS output than threshold exceedances information.

For readability reasons, only a selection of lead times are shown and transparent colors are used to depict the inter-quartile ranges (IQR). We acknowledge that the interpretation of such a graphical representation might require an adaptation time. While we believe that traditional persistence plots are an efficient way to provide a global overview of the situation in a first place, we found these "continuous persistence plots" useful to obtain complementary and deeper insights into the forecasts, for operational work and verification exercises as in this paper.

3.3 Use of scenarios

Under normal conditions, the areas upstream and downstream of the Sihl Lake dam can be considered as uncoupled. About 88% of the inflows to Lake Sihl are used for energy production and released directly into Lake Zurich (Fig. 1). Only weak water amounts are necessary to guarantee the residual water discharge in the downstream part of the basin, as required by the Swiss environmental law. However, during heavy precipitation events, the application of the dam emergency regulation may result in significant water releases into the Sihl. In such situations, the catchment area upstream of the dam contributes greatly to the discharge in Zurich. To explore the consequences of coupling the upstream and downstream areas of the catchment during an extreme event, scenarios were considered. For the two discharge events investigated using continuous persistence plots, the lake balance and the hydraulic model were initialised using an artificially increased Lake Sihl level. For each event, two simulations were started: one forced by interpolated observed meteorological data (HREF-SCEN) and one using the COSMO-LEPS forecast initiated about one day before the peak discharge observed in Zurich (CLEPS-SCEN).

HESSD
8, 715–761, 2011

4 Results and discussion

4.1 Scores

For the Lake Sihl level, COSMO-LEPS and COSMO-7 forecasts show almost equal scores for the shortest lead time (LT1), but performance differences in favor of COSMO-LEPS increase with the time horizon (Table 2). In particular, the COSMO-LEPS LT5 median shows an equally elevated Nash Sutcliffe efficiency value as the COSMO-7 LT3 forecasts. The COSMO-LEPS median is also associated with slightly better results in terms of MAE, but this should not draw off the attention from both models relatively high amplitude of the absolute error which is as high as several centimeters and even reaches 15.9 cm for the COSMO-LEPS LT5 median. A non-negligible error source for the Lake Sihl forecasts stems from uncertainty in the hydropower production. At present, estimates of hydropower production derived from multiple regressions of recent records are used, as the planned hydropower production is confidential and not disclosed. These estimations present an absolute error reaching on average half of the forecast absolute error. Substantial forecast improvements could be achieved if the planned hydropower production could be integrated in real-time model operations.

For forecasts of the Sihl discharge in Zurich, the added-value conveyed by the probability information can be appreciated by comparing the COSMO-LEPS median to the COSMO-7 NSE and MAE (Table 3). For these two scores, using the COSMO-LEPS median instead of the COSMO-7 forecast correspond to a performance gain of 1 to 2 days lead time (COSMO-LEPS LT3 and LT5 are equivalent or better than COSMO-7 LT2 and LT3, respectively). MAE amplitude could be reduced by tuning PREVAH to simulate low flows better. This however would probably be at the expense of the flood forecasting performance (Viviroli et al., 2009c). Positive VOL values indicate a discharge overestimation for both atmospheric models and all lead times, as discussed hereafter. For the metrics considered, the overall performance of the COSMO-LEPS median is better than that of COSMO-7.

HESSD
8, 715–761, 2011

Some key forecasts characteristics are summarized by BSS variations with lead time and discharge threshold (Fig. 4):

- the COSMO-LEPS scores are higher than those achieved forcing PREVAH with COSMO-7 forecasts. This is valid for all lead times and thresholds, and constitutes a quantitative proof of the benefits of running a probability model for the Sihl catchment;
- as expected, BSS reflects the difficulty of correctly forecasting intense events and the decline in weather predictability with increasing lead time. This is depicted by better scores for lower discharge thresholds and generally decreasing values for longer lead times;
- the decrease in performance is faster for COSMO-7 than for COSMO-LEPS, i.e. the "loss of BSS per day of lead time" is smaller for COSMO-LEPS than for COSMO-7. This appears, for instance, clearly for the threshold $Q0.9$. It could indicate a the greater robustness of mid-term probabilistic forecasts thanks to the sampling of the initial atmospheric uncertainties;
- the mid-term forecasts (LT3 to LT5) for the $Q0.9$ and $Q0.99$ thresholds have little skill, and sometimes no skill. This reflects the limited predictability of high discharge events in the small Sihl catchment with the currently available forecasting chain;
- the size of the error bars underlines that the uncertainty in evaluating model performance increases significantly with event intensity. This emphasizes undersampling resulting from the rarity of extreme events.

4.2 Rank histograms

Rank histograms depicting the OBS rank for all days of the time series show overpopulation of the lowest bin (first column in Fig. 5). This denotes recurrent discharge overestimation in Zurich, although this tendency is slightly dampened by increasing lead times. When the HREF rank is depicted (second column), rank uniformity is improved. This suggests that the overestimation originates at least partially from the hydrological model, and affects HREF and COSMO-LEPS forecasts similarly.

When HREF is considered instead of OBS, the histograms switch from an "L-shape" to a "W-shape" (LT1) or a "U-shape" (LT3 and, to a lesser extent, LT5). The population of the two extreme ranks is higher than average which indicates that the COSMO-LEPS atmospheric ensemble tends to be underdispersed. As the ensemble spread usually increases with lead time, less underdispersion is found for LT4 and LT5. There seems to be several reasons for this underdispersion. In particular, the ensemble is coerced by the deterministic initial conditions, so that the spread for the first few hours of the forecast is too narrow. This overconfidence for short-term forecasts is also due to the ECMWF EPS setup, which maximizes the growth of the perturbation total energy in the first 48 h of the forecast (Buizza and Palmer, 1995). As COSMO-LEPS relies on a combination of the two youngest EPS runs (Marsigli et al., 2005), its spread probably needs around two days to develop and reflect atmospheric uncertainty. But it does not explain why underdispersion is still pronounced in LT3 forecasts. The histograms of HREF rank hence show that the corresponding COSMO-LEPS atmospheric forecasts are overall underdispersed. Thus, Marsigli et al. (2008) found that the percentage of outliers for 66-h COSMO-LEPS precipitation forecasts is around twice as high as the theoretical percentage. An overconfidence of COSMO-LEPS-based flow forecasts has been also reported by Renner et al. (2009).

The "W-shape" of the histogram depicting the HREF rank for LT1 can be explained as follows. The comparatively high population of rank 9 is due to the initialization of the ensemble using HREF. If the initialization discharge is the highest discharge of the day for HREF and the 16 members, these 17 simulations will show the same daily maximum. This results in the value 9 (the mean rank among 17 elements) being assigned as the HREF rank. It does not reflect ensemble overdispersion but results from the model setup. It disappears for lead times exceeding 1 day.

HESSD
8, 715–761, 2011

To focus on events of more interest from a flood perspective, only forecasts for days with maximum discharge higher than a selected threshold are considered. However, note that the higher the threshold, the greater the under-sampling. When a threshold selection is applied, the histograms showing OBS rank lose their "L-shape". This suggests that low and middle discharges are overestimated and that such overestimation is probably due to calibration of the hydrological/hydraulic model setup. This may help to explain the VOL observed earlier (Table 3).

The third column (observed discharges exceeding $Q0.9$) in Fig. 5 indicates frequent underdispersion for LT1 forecasts. For LT3 and LT5, the ensemble members tend to underestimate the intensity of larger events, as illustrated by high ranks being more populated than the low ranks (underforecasting bias). This tendency is also reflected in the histograms of the fourth column (observed discharge exceeding $Q0.99$). This implies that the discharges of the most intense events during the study period were associated with relatively low probabilities three to five days before their occurrence. Although this may hinder the effective anticipation of high discharges, more intense events might show earlier warning signs (e.g. Jaun et al., 2008; Thielen et al., 2009b).

For the forecasts of the Lake Sihl level, the two extreme ranks of the histograms are overpopulated for all lead times (not shown). This means that the atmospheric uncertainty, as propagated by HEPS, underestimates the full system uncertainty. In particular, approximations of the hydropower production with multiple regressions represents a large error source, but are not represented by the ensemble spread.

4.3 ROC

ROC indicate that forecast skills in terms of H and FAR decrease with lead time for COSMO-LEPS and COSMO-7 (Fig. 6). Given the comparatively good scores of HREF, this emphasizes that correct atmospheric forecasts are essential for trustworthy discharge forecasts. The diamonds referring to COSMO-7 are located close to COSMO-LEPS ROC for the same lead times, which suggests comparable performance. However, probabilistic forecasts allow end-users to optimize the choice of their warning thresholds according to their economic profile (e.g. Roulin, 2007), which is not possible when using deterministic forecasts.

By increasing the discharge threshold from $Q0.75$ to $Q0.9$, a performance decrease for all lead times and both models is observed. The scores for the threshold $Q0.99$ are not shown because of their very high sampling uncertainty. For the $Q0.90$ threshold, LT2 to LT5 forecasts frequently produce false alarms, which account for roughly 50 to 70% of the warnings. Although end-users are usually more concerned about missed events than by false alarms, these high FAR should be not neglected or trivialized. Unnecessary preventive drawdowns represent significant monetary losses for the dam operators, and successive false alarms could undermine end-users' confidence in the flood forecasting system. The almost vertical inclination of these COSMO-LEPS ROC implies that increasing the probability threshold barely reduces this FAR, but largely penalises the forecasts in terms of H. For the probability threshold 50% (indicated by the central circle on the ROC), mid-term (LT3 to LT5) forecasts perform poorly when capturing observed events ($H \sim 0.35$).

4.4 Reliability diagrams

It was not possible to consider the forecast reliability for each probability threshold because of the limited number of events (see the small effective shown by the sub-plots in Fig. 7 and the important dispersion of the circles). Instead, we tried to capture the dominant tendency using linear regressions. Regression lines for all lead times and both thresholds are mostly located under the diagonal of the plots, with a slope lower than 1. This denotes overforecasting (forecast probability overestimation), which seems to be more accentuated for $Q0.9$ than for $Q0.75$. As a consequence, caution is required when using raw model outputs to assess flood risk in its most basic definition ("probability times consequence") as it might to lead to biased (overestimated) risk estimates for the Sihl catchment.

Discharge overestimation is also indicated by the VOL values presented in Table 3 and by the high FAR shown in Fig. 6. It is probably not solely due to uncertainty in

HESSD
8, 715–761, 2011

assigning calibrated parameter values to PREVAH, but is thought to stem also from COSMO-LEPS' tendency to overforecast precipitation (Marsigli et al., 2008). This bias in precipitation forecasts can be reduced consistently if reforecast techniques (Fundel et al., 2010) are adopted to calibrate the forecasts. Although some experience exists at the European scale (Thielen et al., 2009b), the influence of this bias on the reliability of discharge forecasts still needs to be assessed.

4.5 Insights from the event on 8 August 2007

For both the events chosen, precipitation forecasts were compared to hourly rainfall, measured by the stations shown in Fig. 1. The data were analysed using continuous persistence plots. Theses figures are not included in this paper, but some of the findings are enumerated here in order to better understand the impact of precipitation forecasts on the predicted discharge. Two intense precipitation events on 8 August 2007 triggered the generation of two distinct peak flow events (Fig. 8). A first peak discharge in Zurich was recorded at 09:00 UTC and a second at 23:00 UTC (229 m^3/s, return period of ~18 years). The first phase of intense precipitation peak was missed by COSMO-LEPS and COSMO-7 for all time horizons. Both models performed better in forecasting the second precipitation peak, although they underestimated it for all lead times.

The COSMO-LEPS hydrological forecasts for the day of the event (LT1) showed underdispersion and its spread did not envelope the two discharge peaks (Fig. 8a). The peaks were exceeded by the daily maxima of a single member of the LT2 forecast, indicating an underestimation of the observed peak discharge by most ensemble members. The LT3 forecast missed both peaks. On 9 August, model initialization using HREF (very close to the observed value) explained the good performance of the LT1 forecast. The LT2 and the LT3 forecasts showed higher discharges on 9 August than on the day of the event, but remained overall lower than the observed maximum. COSMO-7 hydrological forecasts also reflected the rather conservative precipitation

HESSD
8, 715–761, 2011

forecasts and are disappointing. The first peak amplitude has been underestimated by at least a factor 3 and the second by at least a factor 2 for all time horizons (Fig. 8b).

The poor hydrological forecasts of this event can be mainly attributed to the atmospheric components of the models chain. This is confirmed by the satisfying agreement between OBS and the HREF run, which captured the timing and the magnitude of both peaks correctly.

4.6 Insights from the event on 15 August 2008

The Sihl discharge in Zurich reached 136 m^3/s at 18:00 UTC on 15 August 2008 (return period of ∼3 years). The correspondence between the COSMO-LEPS precipitation forecasts for 15 August and the observed rainfall increased when going from LT3 to LT1. The forecast initiated the day of the event provided a good approximation of the 24 h cumulated rainfall. However, all forecasts suffered from a rainfall overestimation in the morning. The COSMO-7 cumulated precipitation amounts were lower for LT1 than for antecedent forecasts (LT2 and LT3). Observed amounts were underestimated for the afternoon when the main precipitation event was recorded.

COSMO-LEPS' forecasts of the Sihl discharge increased too early on 15 August (Fig. 9a) because of the precipitation overestimation for the morning. For all the depicted quantiles, the peak discharge gradually increased with decreasing lead times. The forecast initiated at 00:00 UTC on 15 August nicely enveloped the amplitude of the peak discharge, although the observed discharge increase was steeper and occurred a few hours later than forecast. The COSMO-7 forecast with best correspondence to the observed hydrograph is LT3 (Fig. 9b). For this event, COSMO-7 forecasts worsened with decreasing lead time and were clearly outperformed the probabilistic forecasts.

The observed peak discharge amplitude on 15 August 2008 was well captured by HREF, although it was simulated a few hours too late.

HESSD
8, 715–761, 2011

4.7 Scenarios

Given the satisfying correspondence between HREF and the observed discharge for the two analysed events (Figs. 8 and 9), HREF-SCEN is assumed to approximate the discharge that would have been observed if the level of Lake Sihl was of 889.00 m a.s.l. when forecasts were initialized.

In the case of the August 2007 event, the operation limit of the dam (889.34 m a.s.l.) was exceeded by HREF-SCEN for 52 h (Fig. 10). This caused an emergency water release into the Sihl, coupled with a dam overflow whose peak reached 180% of the observed peak discharge at the outlet of the dam (river gauge Schlagen, see Fig. 1). The first inflow peak from the Lake Sihl catchment caused a sharp lake level increase, but most water was retained by the dam. This is indicated by the comparatively low resulting HREF-SCEN discharge at the dam outlet. However, it caused Lake Sihl to reach and exceed the dam operation limit. As a consequence, most of the inflow generated during the second rainfall-runoff event was released into the Sihl. This is supported by the close match between the curves depicting HREF-SCEN discharge in Schlagen and the sum of the Lake Sihl inflows. The peak discharge of the emergency release into the Sihl occurred two hours before the peak observed in Zurich. As the travel time from the dam to Zurich is around three hours for high discharges (Schwanbeck et al., 2007), this release accentuated the observed peak in Zurich. Hence, a situation like HREF-SCEN in August 2007 could have led to a peak runoff of about 325 m^3/s. Such a runoff would have probably caused the flooding of the construction site and large damage to the city of Zurich.

As the forecast evaluation would let us expect, this peak discharge was heavily underestimated by CLEPS-SCEN, principally as a result of the propagation of the precipitation underestimation by COSMO-LEPS (see Sect. 4.5). It caused the lake level to be underestimated, which biased the water release in Schlagen and led to an overly conservative forecast for the Sihl discharge in Zurich. It is probable that if only this forecast for the Sihl discharge in Zurich had been considered, no preventive action

HESSD
8, 715–761, 2011

would have been taken, although it would have been clearly necessary. CLEPS-SCEN did, however, indicate that an exceedance of the dam operation limit and an emergency water release into the Sihl were very probable. In such a situation, producing hydroelectricity at maximum capacity can help to reduce damage by generating additional storage capacity within the reservoir. On 7 August, the daily average discharge for hydroelectricity production was of 6.33 m^3/s, well below the maximum capacity of 26 m^3/s. Similarly, proceeding to a *controlled* lake drawdown before the event can also increase the reservoir storage capacity. This action can moreover decrease the risk of superposition of the peak discharge caused by a defavourable *forced* water release in Schlagen, with the peak generated in the downstream part of the basin. These two mitigation measures could probably have been implemented successfully on the basis of this still imperfect CLEPS-SCEN forecast.

In the case of August 2008 event (Fig. 11), the lake level simulated by HREF-SCEN exceeded the dam operation limit by 14 cm at its maximum. The peak discharge released into the Sihl was 107 m^3/s greater than the observation, and took place when the total Lake Sihl inflows were close to their maximum and almost fully released into the Sihl. Although CLEPS-SCEN forecast the maximum lake level and the peak discharge in Schlagen around four hours too early, it captured their amplitude correctly. HREF-SCEN peak discharge in Schlagen occurred around eight hours *after* the observed peak in Zurich. Hence, the two wave peaks were delayed and did not superimpose. HREF-SCEN peak discharge in Zurich (238 m^3/s) was higher than the observation (136 m^3/s), but probably would have not caused more serious damage than driftwood. Nevertheless, as seven members of CLEPS-SCEN exceeded 300 m^3/s, a preventive lake drawdown would probably have been chosen on the basis of this hypothetical CLEPS-SCEN forecast. It can in this case be argued that CLEPS-SCEN correctly reflected the flooding risk in Zurich, and that it justified the costs of a preventive drawdown.

HESSD
8, 715–761, 2011

4.8 Challenges in decision-making based on hydrometeorological forecasts

The first scenario illustrates how dam overflow can cause serious damage in Zurich and emphasizes the importance of timely controlled water release into the Sihl and modulated hydropower production to reduce the flood risk. Concretely, this implies determining how much and when water should be released to minimize water losses and protecting Zurich. A new module is currently being developed. It consists of an online interface where decision makers can prescribe several drawdown regimes. Re-running the hydraulic model then enables consequences of these scenarios on the peak runoff forecast to be compared. As new atmospheric forecasts become available, the chosen drawdown strategy can be re-evaluated and if necessary adjusted. This adaptive policy should help to manage uncertainties and to contribute to the minimization of water losses for the dam operators and to the reduction of flood damage.

Several studies made use of the cost-loss ratio method to interpret the quality of atmospheric and hydrologic ensemble forecasts in terms of forecast value (Richardson, 2000; Roulin, 2007). This method is a static and probably too simplistic to provide efficient guidance for a situation like the Sihl catchment, which involves several stakeholders with divergent interests, as well as several interrelated mitigation actions. Multi-purpose dam-management, for example based on dynamic programming, could be envisaged to circumvent these limitations (e.g. Faber and Stedinger, 2001; Yao and Georgakakos, 2001; Turgeon, 2005).

Improvements of the system towards decision support might focus on quantitatively assessing whether taking the risk of performing an unnecessary drawdown is justified by an even higher risk of flooding in Zurich. This would require at least two cost-loss functions: one relating the flooding damage in Zurich to the Sihl discharge and one expressing the costs likely to be incurred by the dam operators (losses in energy production) if water is released into the Sihl. The probabilistic hydrological forecasts could be used as input for these two functions to quantify risk. This procedure still presents at least two difficulties for the present case study. First, the reliability diagrams point

HESSD
8, 715–761, 2011

towards a possible overforecasting of the discharge in Zurich. Moreover, too few events are available to assess whether forecasts for extreme discharges are reliable or not. Hence, it seems risky to use raw ensemble output as probabilities. Post-processing of the forecasts before combining them with economic data (e.g. via Bayesian calibration, Reggiani et al., 2009; Raftery et al., 2005) is probably a necessary step towards reliable risk assessment. Second, a quantitative risk estimate and a cost-benefits analysis of the system require the determination of several cost-loss functions for the Sihl catchment. Estimations of flood costs in the city of Zurich are underway and will be available at the earliest in 2011. Until then, only orders of magnitude will be available. It is at present unclear whether precise and accurate risk assessment is necessary for flood mitigation in the Sihl catchment or if robust protection measures can be implemented without reliable models and rather approximate economic information (Dessai et al., 2009).

5 Conclusions and outlook

This study reveals that probability information can be efficiently used by the models chain and delivers useful support for flood mitigation in the Sihl catchment. Multiple deterministic and probabilistic metrics, as well as graphical representations, have been used to evaluate the model chain. The performance of the hydrologic ensemble prediction system is better and decreases less rapidly with lead time than for deterministic forecasts. However, the spread of the weather forecasts is often too low. The hydrological and hydraulic models appear overall to perform well in capturing the amplitude and the timing of the observed peak discharges. The largest source of forecast uncertainty stems from the difficulty of accurately forecasting the intensity, location and timing of intense precipitation events in the relatively small-scale Sihl catchment. Although caution is required because of under-sampling, this seems to limit the ability of mid-term forecasts to confidently and reliably capture observed intense peak discharges. Therefore, although probabilistic forecasts do convey added-value in comparison to deterministic

HESSD
8, 715–761, 2011

ones, precipitation forecasts must be improved to guarantee sufficiently early flood predictions in the Sihl catchment.

The reliability diagrams and false alarm ratios suggest that medium to high discharges tend to be overforecast. This might as well affect extreme discharge forecasts and impede reliable assessment of flood risk. Furthermore, the first high discharge scenario showed that uncontrolled water releases into the Sihl could lead to dramatic damage in Zurich. This advocates for development of a dedicated system to support efficiently decision-making based on hydrological forecasts. Correct streamflow forecasts may not be sufficient for efficient flood mitigation if they are not accompanied by a dedicated tool to compare multiple mitigation actions.

Possible future developments include using calibrated COSMO-LEPS rainfall forecasts (Fundel et al., 2010) to drive the hydrological and hydraulic model. As calibration improves the reliability of precipitation forecasts, it might be beneficial for discharge forecasts as well. Possible combinations of ensemble forecasts with deterministic forecasts (seamless predictions) will also be explored (e.g. Dietrich et al., 2008). COSMO-7 and COSMO2 being more frequently updated than COSMO-LEPS, this could provide time-lagged ensembles of discharge predictions (e.g. Zappa et al., 2008). Such a multi-model approach would give more weight to uncertainties stemming from the formulation of atmospheric models.

This study illustrated the challenge that represent the interpretation and communication of probabilistic forecasts, and their efficient use for decision-making (Demeritt et al., 2007; Bruen et al., 2010). We would like to remember that the framework of this study is a real-life case and not purely experimental. There is a real panel of experts consisting of hydrologists and stakeholders, with the delicate task of making decisions by interpreting the outputs of high-end but nevertheless imperfect models (Badoux et al., 2010). Further real-time experience in dealing with such uncertainties should be gained by the end of the construction of the new railway station below the Sihl River.

Acknowledgements. This study is part of COST-731 (Zappa et al., 2010). The IFKIS-SIHL project is founded by the Department of Waste, Water, Energy and Air (AWEL) of Canton Zurich. The contribution of the WSL to the Sihl experts panel was partly funded by the Swiss Federal Railway (SBB). We are grateful to the Swiss Federal Office of Meteorology and Climatology, MeteoSwiss, and the Swiss Federal Office for the Environment for providing meteorological and hydrological data. Particular thanks are expressed to F. Fundel for his valuable comments and his help regarding bootstrapping techniques. C. Schär is thanked for advising the master thesis of N. Addor, on which this article is based. We are grateful to S. Dingwall for the linguistic revision of the manuscript. The data analysis and visualisation were performed with R (R Development Core Team, 2008).

References

Ambühl, J.: Customer oriented warning systems, Tech. Rep. 84, Veröffentlichung der MeteoSchweiz, 2010. 728

Anderson, J.: A Method for Producing and Evaluating Probabilistic Forecasts from Ensemble Model Integrations, J. Climate, 9, 1518–1530, doi:10.1175/1520-0442(1996)009$\langle$1518:AMFPAE$\rangle$2.0.CO;2, 1996. 728

Badoux, A., Zappa, M., Schatzmann, M., Optlatka, M., Jaun, S., Bösch, M., Gross, M., Steiner, P., Hegg, C., and Rhyner, J.: IFKIS-Hydro Sihl: Beratung, Alarmorganisation und Handlungsmöglichkeiten während dem Bau der Durchmesserlinie beim Hauptbahnhof Zürich, Wasser Energie Luft, 4, 309–320, 2010. 720, 724, 741

Bartholmes, J. C., Thielen, J., Ramos, M. H., and Gentilini, S.: The european flood alert system EFAS - Part 2: Statistical skill assessment of probabilistic and deterministic operational forecasts, Hydrol. Earth Syst. Sci., 13, 141–153, doi:10.5194/hess-13-141-2009, 2009. 718

Bezzola, G. R. and Hegg, C.: Ereignisanalyse Hochwasser 2005, Teil 1 - Prozesse, Schäden und erste Einordnung. Bundesamt für Umwelt BAFU, Eidgenössische Forschungsanstalt WSL, http://www.bafu.admin.ch/publikationen/publikation/00044/, last access: 19 January 2011, vol. 707, Umwelt-Wissen, 2007. 719

Bezzola, G. R. and Hegg, C.: Ereignisanalyse Hochwasser 2005, Teil 2 – Analyse von Prozessen, Massnahmen und Gefahrengrundlagen, Bundesamt für Umwelt BAFU, Eidgenössische Forschungsanstalt WSL, vol. 825, Umwelt-Wissen, http://www.bafu.admin.ch/publikationen/publikation/00100/, last access: 19 January 2011, vol. 825, Umwelt-Wissen, 2008. 719

Bruen, M., Krahe, P., Zappa, M., Olsson, J., Vehvilainen, B., Kok, K., and Daamen, K.: Visualizing flood forecasting uncertainty: some current European EPS platforms – COST731 working group 3, Atoms. Sci. Lett., 11, 92–99, doi:10.1002/asl.258, 2010. 719, 721, 741

Buizza, R. and Palmer, T. N.: The Singular-Vector Structure of the Atmospheric Global Circulation, J. Atmos. Sci., 52, 1434–1456, doi:10.1175/1520-0469(1995)052$⟨$1434:TSVSOT$⟩$ $2.0.CO;2, 1995. 732

Cloke, H. L. and Pappenberger, F.: Ensemble flood forecasting: A review, J. Hydrol., 375, 613–626, doi:10.1016/j.jhydrol.2009.06.005, 2009. 717, 720

Demeritt, D., Cloke, H., Pappenberger, F., Thielen, J., Bartholmes, J., and Ramos, M.: Ensemble predictions and perceptions of risk, uncertainty, and error in flood forecasting, Environmental Hazards, 7, 115–127, doi:10.1016/j.envhaz.2007.05.001, 2007. 741

Dessai, S., Hulme, M., Lempert, R., and Pielke, R. J.: Adapting to climate change: thresholds, values, governance, chap. Climate prediction: a limit to adaptation?, Cambridge University Press, 64–78, 2009. 740

Dietrich, J., Trepte, S., Wang, Y., Schumann, A. H., Voß, F., Hesser, F. B., and Denhard, M.: Combination of different types of ensembles for the adaptive simulation of probabilistic flood forecasts: hindcasts for the Mulde 2002 extreme event, Nonlin. Processes Geophys., 15, 275–286, doi:10.5194/npg-15-275-2008, 2008. 720, 741

Faber, B. A. and Stedinger, J. R.: Reservoir optimization using sampling SDP with ensemble streamflow prediction (ESP) forecasts, J. Hydrol., 249, 113–133, doi:10.1016/S0022-1694(01)00419-X, 2001. 739

Fundel, F., Walser, A., Liniger, M. A., Frei, C., and Appenzeller, C.: Calibrated precipitation forecasts for a limited-area ensemble forecast system using reforecasts, Mon. Weather Rev., 138, 176–189, doi:10.1175/2009MWR2977.1, 2010. 735, 741

Gurtz, J., Baltensweiler, A., and Lang, H.: Spatially distributed hydrotope-based modelling of evapotranspiration and runoff in mountainous basins, Hydrol. Process., 13, 2751–2768, 1999. 723

HESSD
8, 715–761, 2011

Jaun, S. and Ahrens, B.: Evaluation of a probabilistic hydrometeorological forecast system, Hydrol. Earth Syst. Sci., 13, 1031–1043, doi:10.5194/hess-13-1031-2009, 2009. 720

Jaun, S., Ahrens, B., Walser, A., Ewen, T., and Schär, C.: A probabilistic view on the August 2005 floods in the upper Rhine catchment, Nat. Hazards Earth Syst. Sci., 8, 281–291, doi:10.5194/nhess-8-281-2008, 2008. 718, 719, 720, 722, 733

Katz, R. W. and Murphy, A. H.: Economic value of weather and climate forecasts, Cambridge University Press, 1997. 717

Laio, F. and Tamea, S.: Verification tools for probabilistic forecasts of continuous hydrological variables, Hydrol. Earth Syst. Sci., 11, 1267–1277, doi:10.5194/hess-11-1267-2007, 2007. 718

Marsigli, C., Boccanera, F., Montani, A., and Paccagnella, T.: The COSMO-LEPS mesoscale ensemble system: validation of the methodology and verification, Nonlin. Processes Geophys., 12, 527–536, doi:10.5194/npg-12-527-2005, 2005. 717, 721, 722, 732

Marsigli, C., Montani, A., and Paccangnella, T.: A spatial verification method applied to the evaluation of high-resolution ensemble forecasts, Meteorol. Appl., 15, 125–143, doi:10.1002/met.65, 2008. 732, 735

Mason, I.: A model for assessment of weather forecasts, Aust. Meteorol. Mag., 30, 291–303, 1982. 727

Molteni, F., Buizza, R., Palmer, T. N., and Petroliagis, T.: The ECMWF ensemble prediction system: methodology and validation, Q. J. Roy. Meteor. Soc., 122, 73–119, doi:10.1002/qj.49712252905, 1996. 717, 721

Molteni, F., Buizza, R., Marsigli, C., Montani, A., Nerozzi, F., and Paccagnella, T.: A strategy for high-resolution ensemble prediction. I: Definition of representative members and global-model experiments, Q. J. Roy. Meteor. Soc., 127, 2069–2094, doi:10.1002/qj.49712757612, 2001. 721

Murphy, A. H.: Decision Making and the Value of Forecasts in a Generalized Model of the Cost-Loss Ratio Situation, Mon. Weather Rev., 113, 362–369, doi:10.1175/1520-0493(1985)113$⟨$0362:DMATVO$⟩$2.0.CO;2, 1985. 717

Murphy, A. H.: The Finley Affair: A Signal Event in the History of Forecast Verification, Weather Forecast., 11, 3–20, doi:10.1175/1520-0434(1996)011⟨0003:TFAASE⟩2.0.CO;2, 1996. 727

Nash, J. E. and Sutcliffe, J. V.: River forecasting using conceptual models, 1. A discussion of principles, J. Hydrol., 10, 282–290, doi:10.1016/0022-1694(70)90255-6, 1970. 725

HESSD

8, 715–761, 2011

Pappenberger, F., Bartholmes, J., Thielen, J., Cloke, H. L., Buizza, R., and de Roo, A.: New dimensions in early flood warning across the globe using grand-ensemble weather predictions, Geophys. Res. Lett., 35, L10404, doi:10.1029/2008GL033837, 2008.

R Development Core Team: R: A Language and Environment for Statistical Computing, http://www.R-project.org, last access: 20 January 2011, ISBN 3-900051-07-0, 2008. 742

Raftery, A., Gneiting, T., Balabdaoui, F., and Polakowski, M.: Using Bayesian model averaging to calibrate forecast ensembles, Mon. Weather Rev., 133, 1155–1174, 2005. 740

Reggiani, P., Renner, M., Weerts, A. H., and van Gelder, P. A. H. J. M.: Uncertainty assessment via Bayesian revision of ensemble streamflow predictions in the operational river Rhine forecasting system, Water Resour. Res., 45, W02428, doi:10.1029/2007WR006758, 2009. 718, 720, 740

Renner, M., Werner, M. G. F., Rademacher, S., and Sprokkereef, E.: Verification of ensemble flow forecasts for the River Rhine, J. Hydrol., 376, 463–475, doi:10.1016/j.jhydrol.2009.07.059, 2009. 720, 722, 732

Richardson, D. S.: Skill and relative economic value of the ECMWF ensemble prediction system, Q. J. Roy. Meteor. Soc., 126, 649–667, doi:10.1002/qj.49712656313, 2000. 717, 739

Rotach, M. W., Ambrosetti, P., Appenzeller, C., Arpagaus, M., Fontannaz, L., Fundel, F., Germann, U., Hering, A., Liniger, M. A., Stoll, M., Walser, A., Ament, F., Bauer, H.-S., Behrendt, A., Wulfmeyer, V., Bouttier, F., Seity, Y., Buzzi, A., Davolio, S., Corazza, M., Denhard, M., Dorninger, M., Gorgas, T., Frick, J., Hegg, C., Zappa, M., Keil, C., Volkert, H., Marsigli, C., Montaini, A., McTaggart-Cowan, R., Mylne, K., Ranzi, R., Richard, E., Rossa, A., Santos-Muñoz, D., Schär, C., Staudinger, M., Wang, Y., and Werhahn, J.: MAP D-PHASE: Real-Time Demonstration of Weather Forecast Quality in the Alpine Region, B. Am. Meteorol. Soc., 90, 1321–1336, doi:10.1175/2009BAMS2776.1, 2009. 718

Roulin, E.: Skill and relative economic value of medium-range hydrological ensemble predictions, Hydrol. Earth Syst. Sci., 11, 725–737, doi:10.5194/hess-11-725-2007, 2007. 718, 734, 739

Schwanbeck, J., Viviroli, D., Röser, I., Trosch, J., and Weingartner, R.: Prozessbasierte Abschätzung von Extremhochwassern im Einzugsgebiet der Sihl, Schlussbericht zur Studie im Auftrag des Amtes für Abfall, Wasser, Energie und Luft des Kantons Zürich (AWEL), Tech. rep., Veröffentlichung der Universität Bern, 2007. 719, 723, 737

HESSD

8, 715–761, 2011

An operational HEPS for the city of Zurich: skill, case studies and scenarios

N. Addor et al.

Steppeler, J., Doms, G., Schättler, U., Bitzer, H., Gassmann, A., Damrath, U., and Gregoric, G.: Meso-gamma scale forecasts using the nonhydrostatic model LM, Meteorol. Atmos. Phys., 82, 75–96, doi:10.1007/s00703-001-0592-9, 2003. 722

Thielen, J., Bartholmes, J., Ramos, M.-H., and de Roo, A.: The European Flood Alert System - Part 1: Concept and development, Hydrol. Earth Syst. Sci., 13, 125–140, doi:10.5194/hess-13-125-2009, 2009a. 717

Thielen, J., Bogner, K., Pappenberger, F., Kalas, M., Del Medico, M., and de Roo, A.: Monthly-, medium-, and short-range flood warning: testing the limits of predictability, Meteorol. Appl., 16, 77–90, doi:10.1002/met.140, 2009b. 720, 728, 733, 735

Turgeon, A.: Solving a stochastic reservoir management problem with multilag autocorrelated inflows, Water Resour. Res., 41, W12414, doi:10.1029/2004WR003846, 2005. 739

Velázquez, J. A., Petit, T., Lavoie, A., Boucher, M.-A., Turcotte, R., Fortin, V., and Anctil, F.: An evaluation of the Canadian global meteorological ensemble prediction system for short-term hydrological forecasting, Hydrol. Earth Syst. Sci., 13, 2221–2231, doi:10.5194/hess-13-2221-2009, 2009. 718

Verbunt, M., Walser, A., Gurtz, J., Montani, A., and Schär, C.: Probabilistic flood forecasting with a limited-area ensemble prediction system: selected case studies, J. Hydrometeorol., 8, 897–909, doi:10.1175/JHM594.1, 2007. 718

Viviroli, D., Mittelbach, H., Gurtz, J., and Weingartner, R.: Continuous simulation for flood estimation in ungauged mesoscale catchments of Switzerland - Part II: Parameter regionalisation and flood estimation results, J. Hydrol., 377, 208–225, doi:10.1016/j.jhydrol.2009.08.022, 2009a. 723

Viviroli, D., Zappa, M., Gurtz, J., and Weingartner, R.: An introduction to the hydrological modelling system PREVAH and its pre-and post-processing-tools, Environ. Modell. Softw., 24, 1209–1222, doi:10.1016/j.envsoft.2009.04.001, 2009b. 723

Viviroli, D., Zappa, M., Schwanbeck, J., Gurtz, J., and Weingartner, R.: Continuous simulation for flood estimation in ungauged mesoscale catchments of Switzerland – Part I: Modelling framework and calibration results, J. Hydrol., 377, 191–207, doi:10.1016/j.jhydrol.2009.08.023, 2009c. 723, 730

Weigel, A. P., Liniger, M. A., and Appenzeller, C.: The Discrete Brier and Ranked Probability Skill Scores, Mon. Weather Rev., 135, 118–124, doi:10.1175/MWR3280.1, 2007. 727

Wilks, D.: Statistical Methods in the Atmospheric Sciences, vol. 91 of International geophysics series, Elsevier, New York, 2006. 725, 726, 728

HESSD

8, 715–761, 2011

An operational HEPS for the city of Zurich: skill, case studies and scenarios

N. Addor et al.

Yao, H. and Georgakakos, K. P.: Assessment of Folsom lake response to historical and potential future climate scenarios: 2. Reservoir management, J. Hydrol., 249, 176–196, doi:10.1016/S0022-1694(01)00418-8, 2001. 739

Zappa, M. and Kan, C.: Extreme heat and runoff extremes in the Swiss Alps, Nat. Hazards Earth Syst. Sci., 7, 375–389, doi:10.5194/nhess-7-375-2007, 2007. 725

Zappa, M., Rotach, M. W., Arpagaus, M., Dorninger, M., Hegg, C., Montani, A., Ranzi, R., Ament, F., Germann, U., Grossi, G., Jaun, S., Rossa, A., Vogt, S., Walser, A., Wehrhan, J., and Wunram, C.: MAP D-PHASE: real-time demonstration of hydrological ensemble prediction systems, Atoms. Sci. Lett., 9, 80–87, doi:10.1002/asl.183, 2008. 718, 741

Zappa, M., Beven, K., Bruen, M., Cofino, A., Kok, K., Martin, E., Nurmi, P., Orfila, B., Roulin, E., Schroeter, K., Seed, A., Stzurc, J., Vehvilaeinen, B., Germann, U., and Rossa, A.: Propagation of uncertainty from observing systems and NWP into hydrological models: COST-731 Working Group 2, Atmos. Sci. Lett., 11, 83–91, doi:10.1002/asl.248, 2010. 742

Zappa, M., Schwanbeck, J., Badoux, A., Jaun, S., Röser, I., Schatzmann, M., Walser, A., Vogt, S., Liechti, K., Addor, N., , Viviroli, D., Steiner, P., Trösch, J., Weingartner, R., Bösch, M., Optlatka, M., Hegg, C., and Rhyner, J.: Seamless information for flood mitigation measures with up to five days lead time: an operational implementation for the city of Zurich (Switzerland), Nat. Haz. Earth. Sys., in preparation, 2011.

Zhu, Y., Toth, Z., Wobus, R., Richardson, D., and Mylne, K.: The Economic Value Of Ensemble-Based Weather Forecasts, B. Am. Meteorol. Soc., 83, 73–83, doi:10.1175/1520-0477(2002)083$⟨$0073:TEVOEB$⟩$2.3.CO;2, 2002. 717, 727

HESSD

8, 715–761, 2011

Table 1. Thresholds for the Sihl discharge in Zurich considered for models evaluation.

	Quantile	Discharge (m^3/s)	Average frequency
$Q0.75$	75th	9.1	Every four days
$Q0.9$	90th	21.18	Three times a month
$Q0.99$	99th	73.13	~ every three months

HESSD
8, 715–761, 2011

Table 2. Nash Sutcliffe efficiency NSE (–) and mean absolute error MAE (cm) for the daily maximum of the Lake Sihl level. HREF reflects the skill of the hydrological/hydraulic part of the models chain. Forecasts based on COSMO-LEPS median (CLm) and COSMO-7 (C7) are evaluated for lead times (LT) of 1 to 5, and 1 to 3 days, respectively.

	HREF	LT1	LT2	LT3	LT4	LT5
NSE CLm	0.84	0.65	0.65	0.58	0.52	0.46
NSE C7		0.64	0.56	0.46	–	–
MAE CLm	1.7	2.4	5.9	9.2	12.5	15.9
MAE C7		2.4	6.3	10.1	–	–

HESSD
8, 715–761, 2011

Table 3. Nash Sutcliffe efficiency NSE (–), mean absolute error MAE (m^3/s) and volume error VOL (%) for the Sihl discharge in Zurich. The notation conventions are the same as in Table 2.

	HREF	LT1	LT2	LT3	LT4	LT5
NSE CLm	0.87	0.70	0.44	0.25	0.20	0.10
NSE C7		0.55	0.20	−0.09	–	–
MAE CLm	3	3.9	5.2	5.6	6	6.3
MAE C7		4.1	5.7	6.2	–	–
VOL CLm	17	18	18	12	9	3
VOL C7		12	7	12	–	–

HESSD
8, 715–761, 2011

HESSD

8, 715–761, 2011

An operational HEPS for the city of Zurich: skill, case studies and scenarios

N. Addor et al.

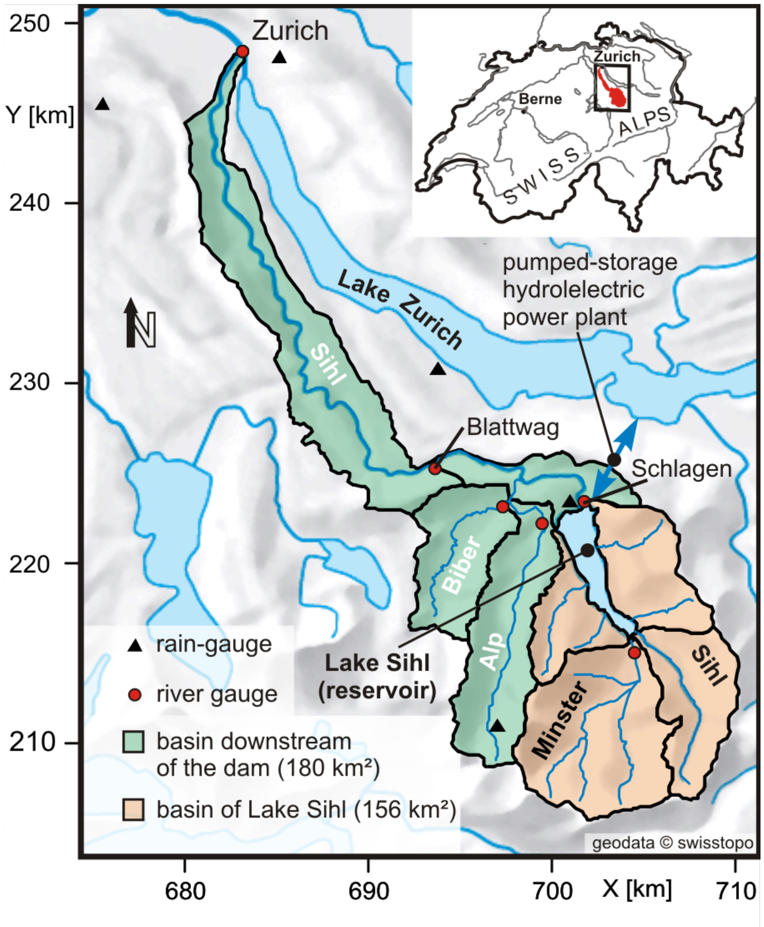

Fig. 1. Map of the Sihl catchment. The nine sub-catchments and the available measuring stations are shown. Courtesy of J. Schwanbeck, University of Bern.

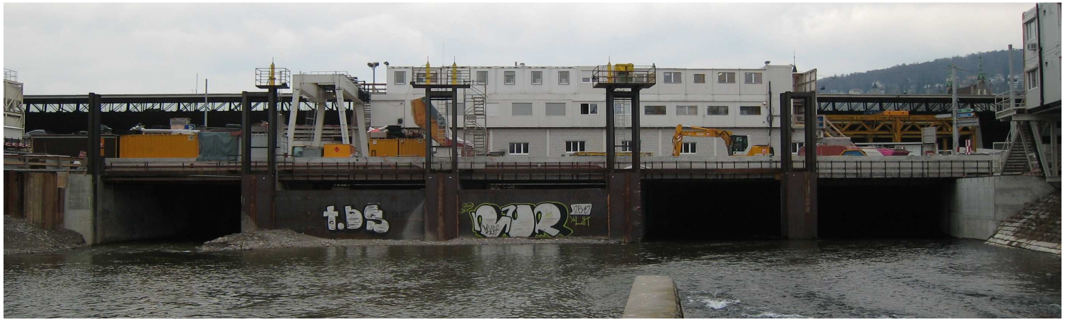

Fig. 2. The Sihl River flows beneath Zurich central railway station. Two of the five channels are currently sealed to provide dry conditions for the construction site located under the river level. The mean discharge on the day of the picture was 8.92 m^3/s. Photo courtesy of A. Badoux, WSL.

HESSD
8, 715–761, 2011

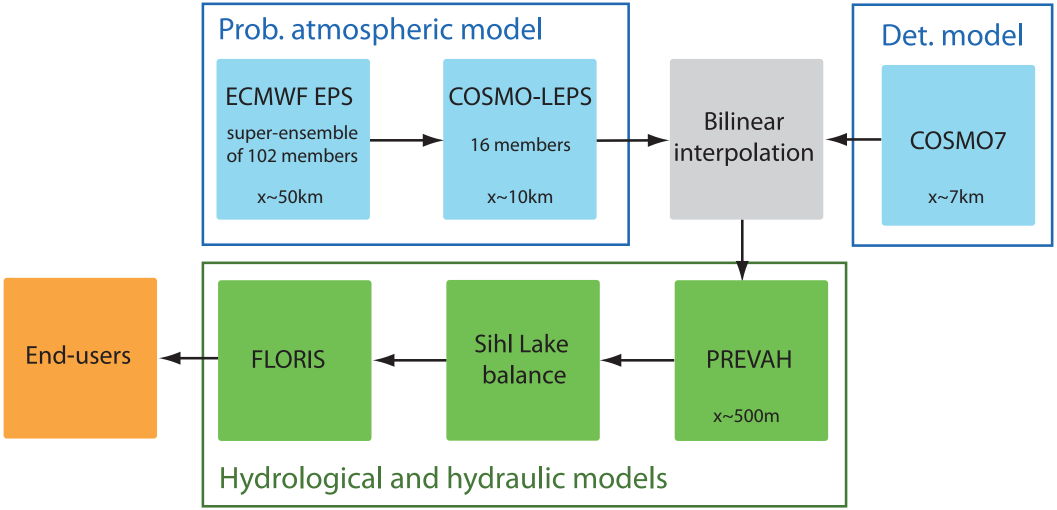

Fig. 3. Flowchart of the prediction chain, illustrating in particular that probability (prob.) and deterministic (det.) atmospheric forecasts are used to force the hydrological model. The model's horizontal grid spacing is denoted by x and indicates that atmospheric forecasts are downscaled throughout the chain.

HESSD
8, 715–761, 2011

An operational HEPS for the city of Zurich: skill, case studies and scenarios

N. Addor et al.

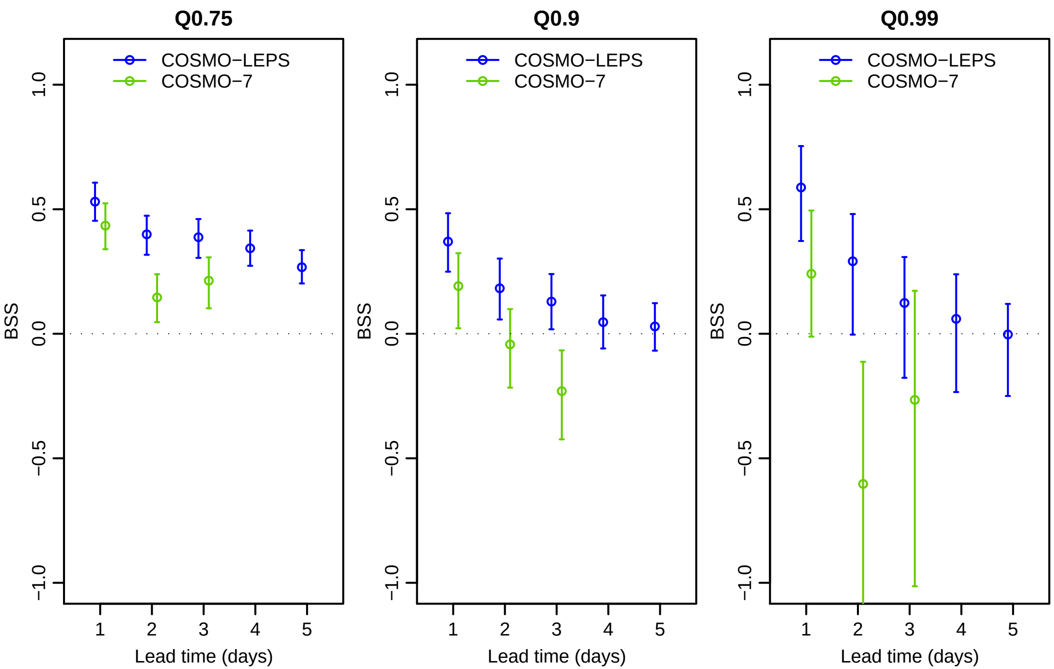

Fig. 4. Brier skill scores (BSS) for COSMO-LEPS and COSMO-7 based forecasts for the daily maximum Sihl discharge in Zurich. Scores for the discharge thresholds $Q0.75$, $Q0.9$ and $Q0.99$ are shown from left to right. The circles exhibit the raw BSS, while the extremities of the confidence intervals consist of the 5th and 95th quantiles derived by bootstrapping.

HESSD
8, 715–761, 2011

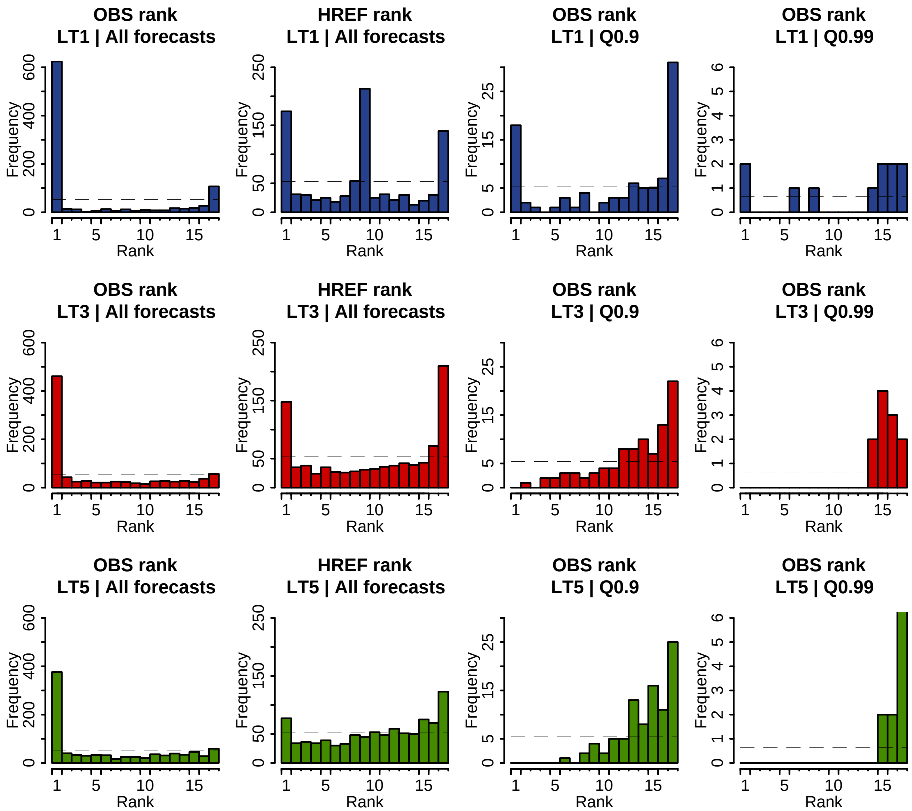

Fig. 5. Rank histograms for the daily maximum Sihl discharge in Zurich. The rank of OBS or HREF, within the 16 daily maxima forecast by the ensemble members, is depicted for lead times of 1, 3 and 5 days. Histograms of the two first columns are based on the whole time series. For the two last columns, only days with an observed discharge exceeding $Q0.9$ and $Q0.99$, respectively, are included. Perfect rank uniformity is indicated by the horizontal dashed line.

HESSD
8, 715–761, 2011

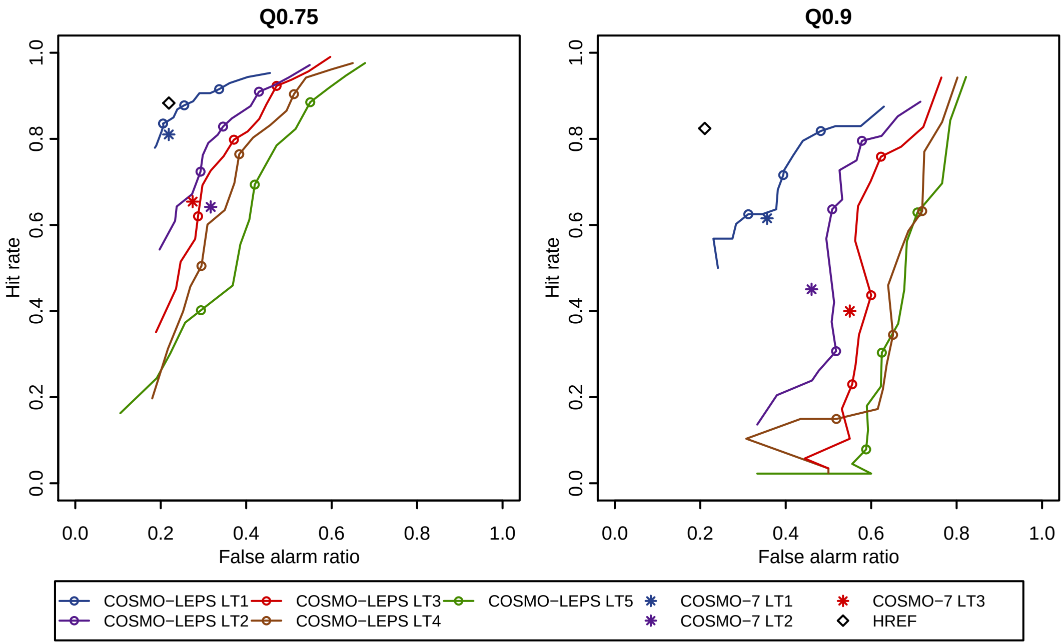

Fig. 6. False alarm ratio and hit rate for the daily maximum Sihl discharge in Zurich for the discharge thresholds $Q0.75$ (left) and $Q0.9$ (right). The lines (ROC) refer to COSMO-LEPS forecasts. The stars and diamonds indicate COSMO-7 and HREF performance, respectively. Circles on the ROC refer to the probability thresholds 25%, 50% and 75% (from right to left).

HESSD
8, 715–761, 2011

An operational HEPS for the city of Zurich: skill, case studies and scenarios

N. Addor et al.

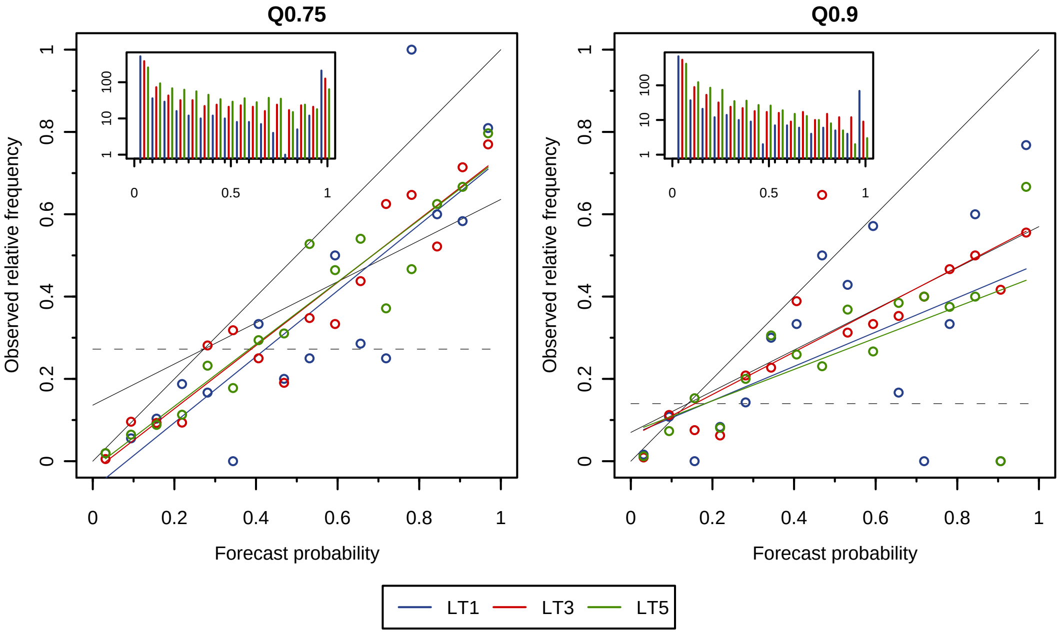

Fig. 7. Reliability diagrams for the daily maximum Sihl discharge in Zurich for the discharge thresholds $Q0.75$ (left) and $Q0.9$ (right). The circles indicate the observed frequency of each forecast probability class for lead times of 1, 3 and 5 days. A linear regression is depicted for each lead time. The sub-plots show the associated refinement distributions.

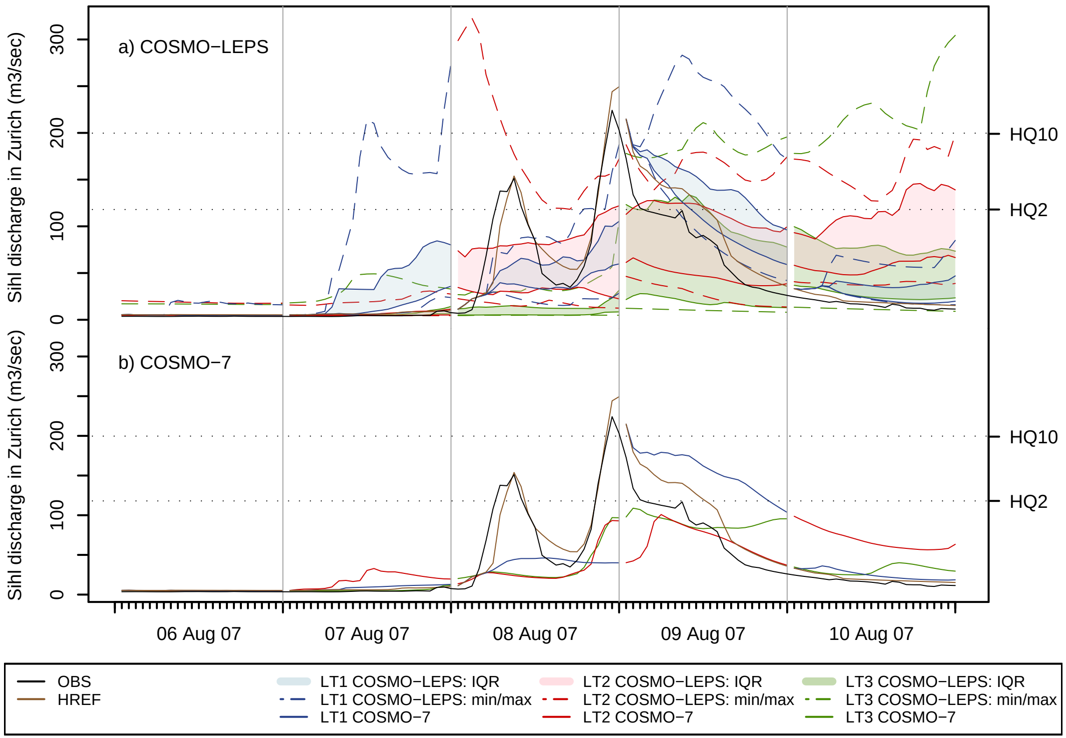

Fig. 8. Continuous persistence plots centered on the 8 August 2007 event depicting the discharge in Zurich. COSMO-LEPS-based **(a)** and COSMO-7-based forecasts **(b)** are shown for lead times of 1, 2 and 3 days. The vertical gray lines indicate 00:00 UTC. Discharges associated with return periods of 2 and 10 years are depicted by the horizontal dotted lines, HQ2 and HQ10, respectively.

HESSD
8, 715–761, 2011

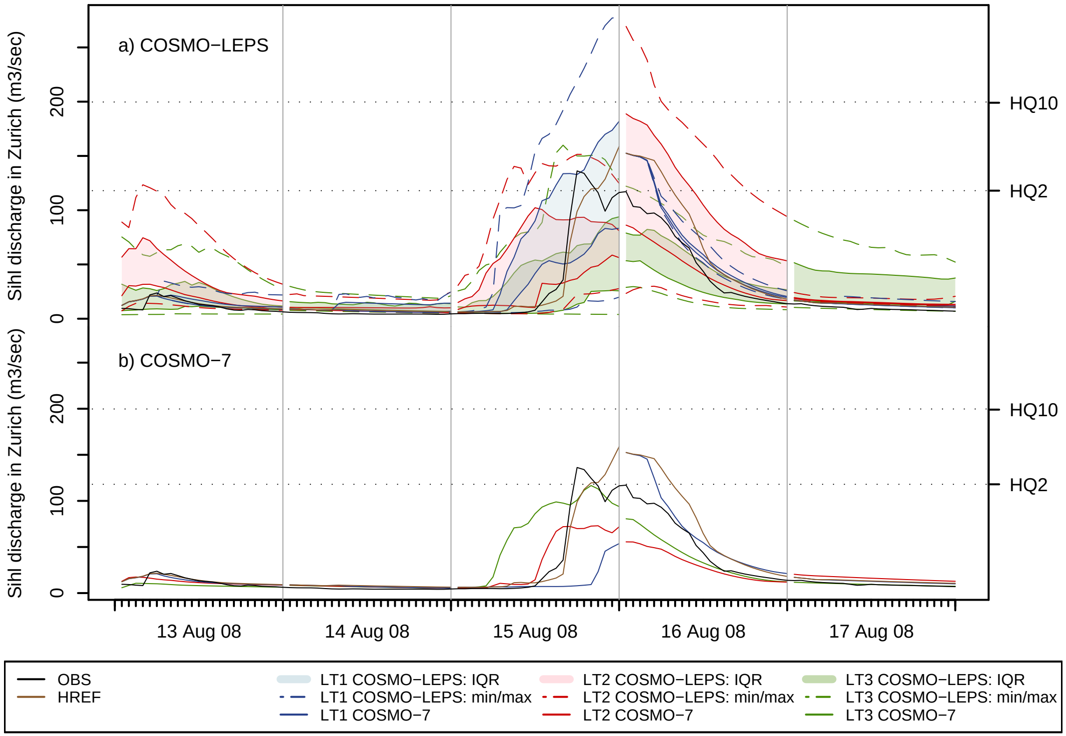

Fig. 9. Continuous persistence plots as in Fig. 8, but centered on the 15 August 2008 event.

HESSD
8, 715–761, 2011

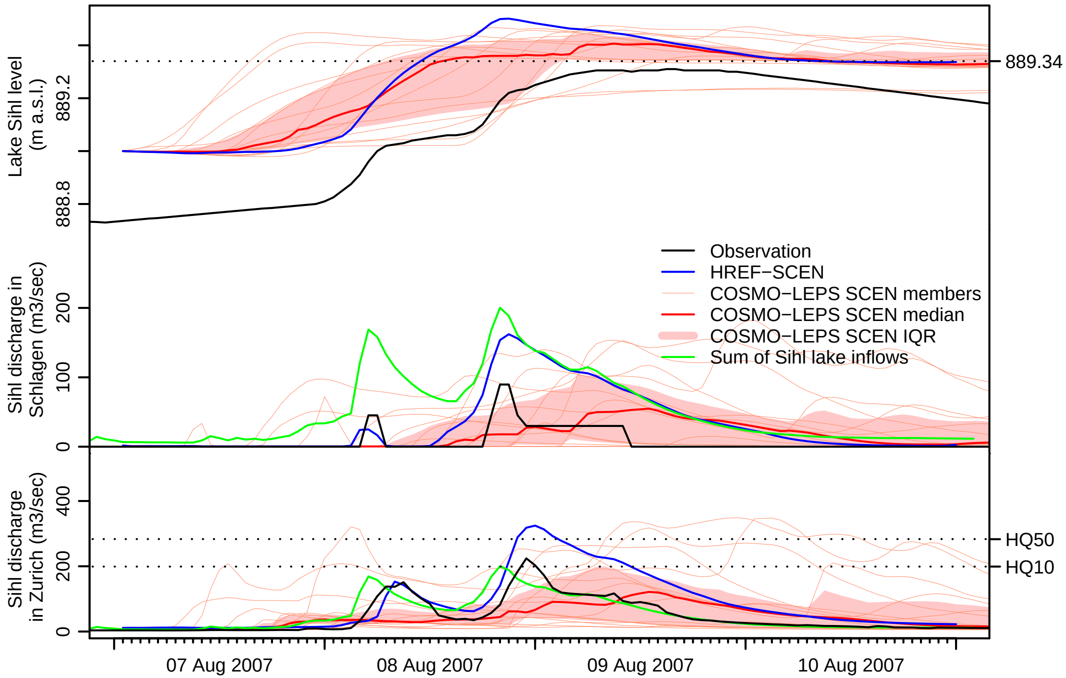

Fig. 10. Lake Sihl level (top), water released at the dam outlet (Schlagen, center) and discharge in Zurich (bottom) for an artificially increased Sihl Lake level of 889 m a.s.l. on the 7 August 2007 at 00:00 UTC. Dotted lines indicate the altitude of the dam operation limit (889.34 m a.s.l., top plot) and the discharges associated with return periods of 10 and 50 years (HQ10 and HQ50, bottom plot).

HESSD
8, 715–761, 2011

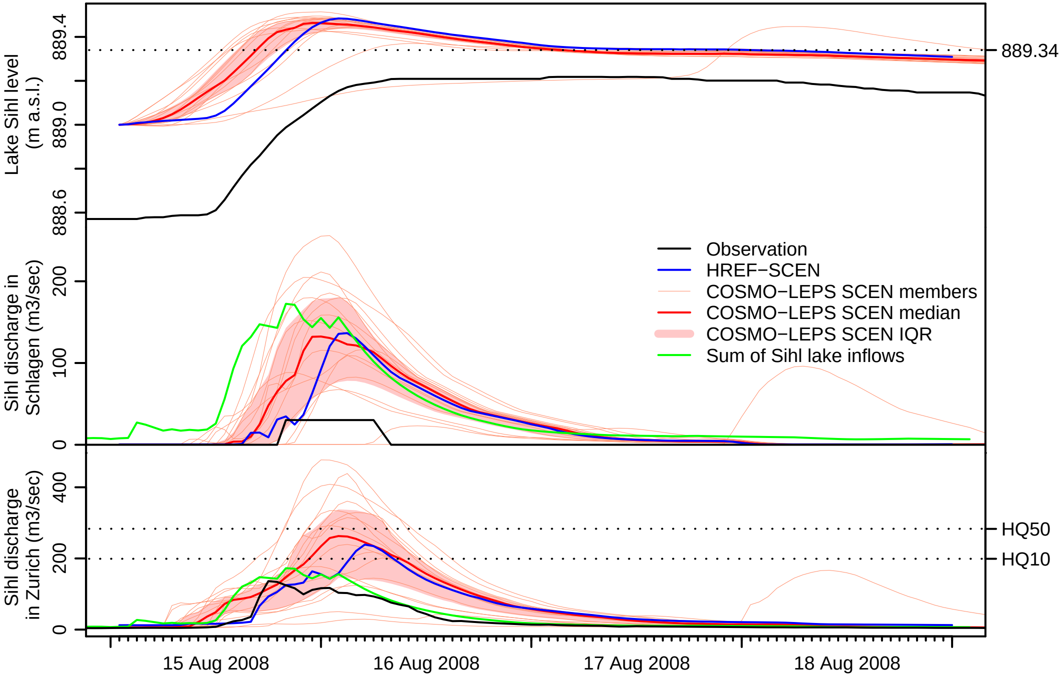

Fig. 11. As in Fig. 10, but for an artificially increased Sihl Lake level of 889 m a.s.l. on 15 August 2008 at 00:00 UTC.

HESSD
8, 715–761, 2011